

# The Stimulatory Potency of T Cell Antigens Is Influenced by the Formation of the Immunological Synapse

Sašo Čemerski,<sup>1,6</sup> Jayajit Das,<sup>3,6</sup> Jason Locasale,<sup>4</sup> Phoebe Arnold,<sup>1</sup> Emanuele Giurisato,<sup>1</sup> Mary A. Markiewicz,<sup>1</sup> Daved Fremont,<sup>1,2</sup> Paul M. Allen,<sup>1</sup> Arup K. Chakraborty,<sup>3,4,5,\*</sup> and Andrey S. Shaw<sup>1,\*</sup>

<sup>1</sup>Department of Pathology

<sup>2</sup>Department of Biochemistry and Molecular Biophysics  
Washington University School of Medicine, St. Louis, MO 63110

<sup>3</sup>Department of Chemical Engineering

<sup>4</sup>Division of Biological Engineering

<sup>5</sup>Department of Chemistry

Massachusetts Institute of Technology, Cambridge, MA 02139

<sup>6</sup>These authors contributed equally to this work.

\*Correspondence: [arupc@mit.edu](mailto:arupc@mit.edu) (A.K.C.), [ashaw@wustl.edu](mailto:ashaw@wustl.edu) (A.S.S.)

DOI 10.1016/j.immuni.2007.01.013

## SUMMARY

T cell activation is predicated on the interaction between the T cell receptor and peptide-major histocompatibility (pMHC) ligands. The factors that determine the stimulatory potency of a pMHC molecule remain unclear. We describe results showing that a peptide exhibiting many hallmarks of a weak agonist stimulates T cells to proliferate more than the wild-type agonist ligand. An *in silico* approach suggested that the inability to form the central supramolecular activation cluster (cSMAC) could underlie the increased proliferation. This conclusion was supported by experiments that showed that enhancing cSMAC formation reduced stimulatory capacity of the weak peptide. Our studies highlight the fact that a complex interplay of factors determines the quality of a T cell antigen.

## INTRODUCTION

The activation of T cells is stimulated by the binding of the T cell receptor (TCR) to its ligand, short peptides (p) bound to major histocompatibility (MHC) gene products. Initially it was thought that each TCR was specific for a single pMHC molecule, but it is now clear that a variety of related peptides can stimulate signaling through a particular TCR. The specific sequence of a peptide determines its stimulatory ability and the resulting functional outcome.

Altered peptide ligands (APLs), generated by mutating residues of the wild-type agonist peptide, have been used to investigate the role of antigen quality on T cell activation as well as mechanisms underlying TCR signaling (Evavold et al., 1993). APLs can have enhanced or reduced stimulatory ability compared to the wild-type (WT)

agonist peptide. The stimulatory potency of a peptide has been correlated with a variety of parameters that include the dissociation rate of the TCR-pMHC complex, the ability to downregulate TCRs, the ability to form an immunological synapse (IS), and the ability to generate fully phosphorylated TCR- $\zeta$  chains (Bachmann et al., 1997; Grakoui et al., 1999; Itoh et al., 1999; Kersh et al., 1998a; Madrenas et al., 1995; Sloan-Lancaster et al., 1994; Valitutti et al., 1995). The importance of the density of antigenic pMHC molecules expressed on an APC has also been noted (Gonzalez et al., 2005). How each of these parameters is linked to biophysical features of the TCR-pMHC interaction, stimulatory potency, and T cell signaling is not clearly understood. In this paper, we try to parse some of these connections by studying the relationship between TCR-pMHC binding parameters, formation of the IS, and T cell signaling and activation. For these studies, we stimulated AND TCR transgenic T cells (which recognize the moth cytochrome C (MCC) peptide presented by I-E<sup>k</sup> [Kaye et al., 1989]) with a series of APLs.

The IS refers to the spatially organized motif of membrane proteins and cytosolic molecules that forms at the junction between a T cell and an antigen-presenting cell (APC) (Grakoui et al., 1999; Monks et al., 1998). In some ISs, TCR and pMHC ligands are clustered in the center of the contact area (a structure called the cSMAC). In spite of numerous studies, the function of the cSMAC remains elusive (e.g., Grakoui et al., 1999; Monks et al., 1998; Campi et al., 2005; Lee et al., 2002, 2003; Lin et al., 2005; Yokosuka et al., 2005).

We combined *in vitro* experiments with computational studies to examine how TCR signaling may be influenced by the biophysical parameters characterizing TCR-pMHC binding and cSMAC formation. The computational results show that, for pMHC ligands that bind the TCR with a sufficiently long half-life, the primary function of the cSMAC is to enhance TCR downregulation. One surprising consequence of this effect is our finding that a weak pMHC

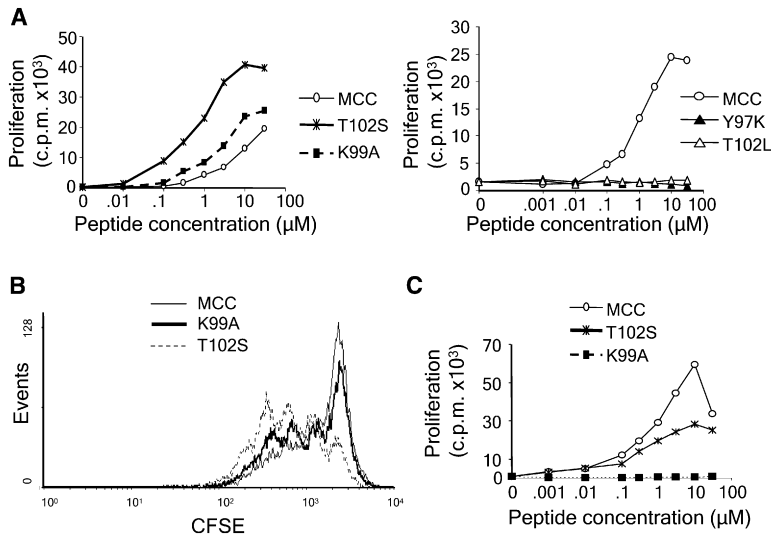


**Figure 1. Proliferative Response of AND and 5C.C7 T Cells to WT and Altered MCC Peptides**

AND CD4<sup>+</sup> T cells (A and B) and 5C.C7 CD4<sup>+</sup> T cells (C) were isolated from spleens of TCR transgenic mice and stimulated with irradiated B10.BR splenocytes and the indicated peptides for 72 hr.

(A and C) The T cell proliferative response was assessed by the incorporation of [<sup>3</sup>H]thymidine added for the last 18 hr of the stimulation. A representative of 10 individual experiments is shown.

(B) AND T cells were CFSE labeled and stimulated for 3 days with irradiated B10.BR splenocytes loaded with 1 μM of the indicated peptides. The T cell proliferative response was assessed by CFSE dilution. A representative of three individual experiments is shown.

ligand that does not induce cSMAC formation results in enhanced T cell proliferation compared to the wild-type agonist. To prove that inability to induce cSMAC formation underlies the hyperproliferative response, we used NKG2D, a receptor expressed on NK cells and some CD8 T cells that can enhance cSMAC formation regardless of antigen quality (Markiewicz et al., 2005), and we found that cSMAC formation inhibited the stimulatory capacity of the weak peptide agonist. Our computational studies, however, also indicated that currently available data cannot unequivocally conclude that the cSMAC always inhibits T cell signaling and activation. Future experimentation that could help resolve this issue are suggested.

## RESULTS

### Identification of APLs for AND T Cells

To determine the relationship between antigen quality, IS formation, and signaling, we used T cells from the AND TCR transgenic mouse (Kaye et al., 1989). This TCR recognizes the MCC 88–103 peptide presented by I-E<sup>k</sup>. Although the stimulatory potency of a range of peptides obtained by mutating residues of MCC is known for the other cytochrome C TCR transgenic systems (Berg et al., 1989; Lyons et al., 1996; Matsui et al., 1994; Reay et al., 1994; Seder et al., 1992; Wulfig et al., 1997), APLs for AND were less well defined. We therefore tested the ability of several variants of the MCC peptide (including T102S, K99A, Y97K, and T102L) to stimulate AND T cells. Two of the peptides, Y97K and T102L, were previously known to behave as null peptides for AND (Rogers et al., 1998).

First, we tested each peptide for its ability to induce T cell proliferation. Naive T cells were stimulated with WT or mutated MCC peptides, and T cell proliferative responses were measured by both [<sup>3</sup>H]thymidine uptake and CFSE dilution. As expected, the two null peptides, Y97K and T102L, did not induce any T cell proliferation

(Figure 1A, right). T102S and K99A both induced a stronger T cell proliferative response than WT MCC peptide (Figure 1A, left). Results from CFSE-dilution experiments were consistent with the thymidine incorporation data (Figure 1B). We excluded the possibility that these differences were related to differences in activation-induced cell death by measuring the percentages of live and dead cells as well as by staining with annexin V (see Figure S1 in the Supplemental Data available online). These results suggest that both the K99A and T102S peptides function as strong agonists.

We confirmed the identity of the peptides by assessing the proliferative response of T cells to these same peptides in another MCC-specific TCR transgenic model, the 5C.C7 TCR (Seder et al., 1992). As expected, T102S and K99A behaved as a weak agonist and a null peptide, respectively, for 5C.C7 T cells (Figure 1C; Lyons et al., 1996; Reay et al., 1994; Wulfig et al., 1997). Thus, T102S and K99A peptides induce a more robust T cell proliferative response than does the WT MCC peptide.

### Determining Dissociation Kinetics and Relative Affinities of WT, K99A, and T102S MCC Peptides

To determine the relative affinities of MCC, K99A, and T102S for the AND TCR, we generated I-E<sup>k</sup> tetramers with each of the peptides and analyzed the equilibrium tetramer staining of AND T cells by flow cytometry. Although WT and T102S showed comparable tetramer binding at the same dose, the amount of K99A tetramer staining of AND T cells was much lower (Figure 2A). This suggested that I-E<sup>k</sup>-K99A has a lower relative affinity for the AND TCR compared to the WT and T102S-loaded I-E<sup>k</sup> complexes.

Because differences in affinity for the TCR are often related to the off rates characterizing TCR-pMHC binding, a tetramer decay assay was performed to determine the relative off rates for MCC, K99A, and T102S. AND T cells were incubated with the three tetramers, and tetramer

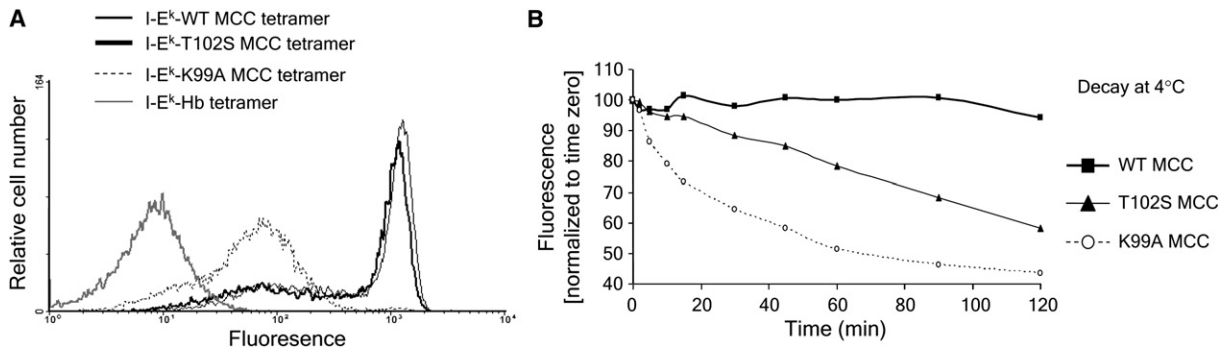


**Figure 2. Staining of AND Cells with I-E<sup>k</sup> Tetramers Presenting MCC and Its APLs**

Naive CD4<sup>+</sup> AND T cells were stained with the indicated tetramers for 3 hr at 4°C (in azide-containing buffer) and with anti-CD8-FITC and anti-B220-CyChrome during the last 30 min, and washed 3 times in ice-cold FACS buffer.

(A) Samples were immediately analyzed by flow cytometry.

(B) Samples were resuspended in FACS buffer with 100 μg/ml of 14.4.4 antibody and incubated at 4°C. At indicated time points, aliquots were taken and analyzed by flow cytometry for tetramer staining. Gate was set on FS/SS bright, CD8<sup>+</sup> and B220<sup>+</sup> cells. A representative of three independent experiments is shown.

disassociation was monitored by flow cytometry over 2 hr. The T102S and K99A tetramers disassociated much faster than the tetramers containing the WT peptide (Figure 2B). Thus, these results suggest that complexes of T102S and K99A pMHC with the AND TCR have a shorter apparent half-life compared to the WT MCC peptide. In addition, although we do not have a measurement of the on rate, combining the relative affinity measurements with the results of the tetramer decay experiments suggests that T102S binds the AND TCR with a larger on rate compared to MCC.

#### TCR Downregulation and Degradation

The paradoxical finding that the T102S and K99A peptides have faster off rates but stimulate a stronger proliferative response led us to examine other measures of agonist quality, such as the ability to induce TCR downregulation and degradation (Bachmann et al., 1997; Itoh et al., 1999; Valitutti et al., 1995). I-E<sup>k</sup>-expressing CH27 cells were loaded with a range of peptide concentrations and incubated with T cells, and TCR downregulation was assessed by flow cytometry. The WT and T102S peptides both induced a dose-dependent downregulation of the TCR (Figure 3A). In contrast, K99A induced low downregulation, and the Y97K and T102L peptides induced essentially none (Figure 3A). Consistent with the idea that TCR downregulation is due to degradation, immunoblotting for TCR-ζ chains showed that the WT and T102S peptides induced markedly greater TCR degradation compared to the K99A peptide (Figure 3B). Thus, although K99A induces a strong T cell proliferative response, surprisingly, it induces poor TCR downregulation and degradation like a weak agonist.

#### Antigen-Induced IS and cSMAC Formation

We next evaluated the ability of these peptides to induce conjugate formation, IS formation, and cSMAC formation. To assess conjugate formation, T cells and peptide-loaded CH27 cells were labeled with two different colored

dyes, incubated together for 30 min, and quantitated by flow cytometry. Conjugate formation between T cells and APCs loaded with T102S, K99A, and WT MCC was comparable and higher than conjugate formation with APCs without peptide or loaded with a null peptide (Figure 4A).

To assess IS and cSMAC formation in T cell-APC conjugates, AND T cells were transduced with a retrovirus encoding TCR-ζ-GFP (Krummel et al., 2000) or doubly transduced with retroviruses encoding CD11a-YFP and CD28-CFP. After sorting, cells were incubated with APCs preloaded with peptides, and conjugates were fixed and analyzed for IS and cSMAC formation. Conjugates were scored as having formed an IS if the mean fluorescence of the cSMAC marker, TCR-ζ, or CD28 at the contact site was at least two times higher than the mean fluorescence of the rest of the T cell membrane (Figure 4B and Figure S2). Conjugates were scored as cSMAC positive if there was an area of the contact site, not bigger than one-third of the contact site, that had at least a two-fold enrichment of TCR-ζ or CD28 (Figure 4B and Figure S2). In the doubly transduced cells, we also confirmed that when the cSMAC formed, CD28 accumulated in the center and lacked the pSMAC marker, CD11a (Figure S2). Finally, conjugates with no obvious TCR-ζ or CD28 accumulation at the contact site were scored as negative (Figure 4B and Figure S2).

The percentage of IS-positive conjugates was highest for the T102S peptide, followed by the WT peptide, and then by the K99A peptide (Figure 4C). Scoring the conjugates for cSMAC formation revealed a similar pattern with cSMACs forming most readily with T102S, followed by MCC, and then by K99A (Figure 4D and Figure S2A). Finally, the reduced ability of K99A to form a mature IS was also seen when T cells were incubated on lipid bilayers (Figure S3). Taken together, our results suggest that ability to efficiently form cSMACs does not always correlate with the stimulatory capacity of the peptide.

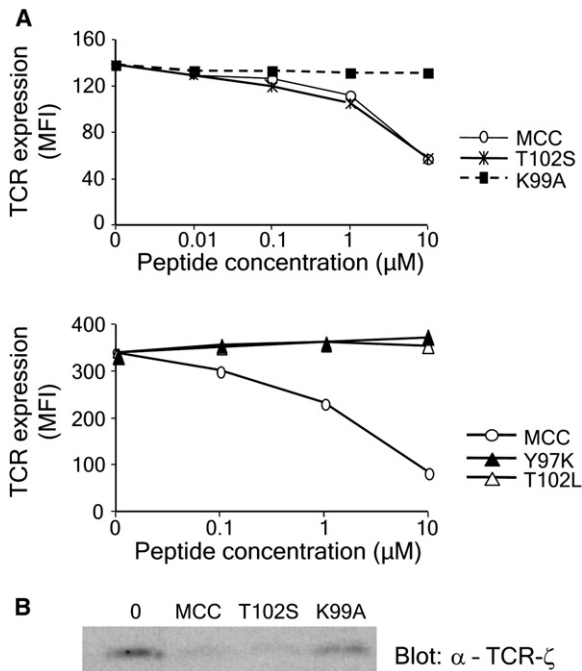


**Figure 3. TCR Downregulation and Degradation in AND T Cells Stimulated with WT and APLs for MCC 88–103 Peptide**  
 (A) CD4<sup>+</sup> T cells were purified from AND TCR tg mice spleens and stimulated for 3 hr with CH27 cells loaded with increasing amounts of the indicated peptides. Upon stimulation, cell conjugates were disrupted by trypsin-EDTA treatment and cells were stained with anti-Vβ3 and anti-CD4, washed, and analyzed by flow cytometry for surface TCR expression. A representative of seven independent experiments is shown.  
 (B) Rested AND CD4<sup>+</sup> T cells were pretreated for 45 min with cyclohexamide and subsequently stimulated for 3 hr with CH27 cells loaded with 30 μM of the indicated peptide. Upon stimulation, cells were lysed and TCR-ζ expression was assessed by immunoblotting. A representative of three independent experiments is shown.

### Full and Partial TCR-ζ Phosphorylation

Another indicator of agonist quality is the ratio of fully (p23) to partially (p21) phosphorylated TCR-ζ chains (Madrenas et al., 1995; Sloan-Lancaster et al., 1994). Stimulation with stronger agonists is thought to lead to a greater proportion of fully phosphorylated receptors and is reflected in the ratio of p23/p21 TCR-ζ phosphorylated forms. T cells were stimulated with APCs loaded with the K99A, T102S, and WT MCC peptides. Compared to stimulation with the WT MCC peptide, both T102S and K99A showed lower p23/p21 ratios (Figure 5A).

The time course of TCR-ζ phosphorylation over 1 hr revealed differences in the kinetics of phosphorylation. Although the WT MCC peptide induced a fast increase in TCR-ζ phosphorylation that attenuated rapidly (Figure 5B), stimulation with both K99A and T102S was prolonged and detectable even after 1 hr of stimulation (Figure 5A). Similar results were obtained when lysates were stained for activated ERK (Figure S4). The prolonged kinetics of signaling was specific for the peptide, as indicated by the fact that it was detectable even with 1% peptide loaded

(data not shown). Lastly, the overall amount of ζ-phosphorylation was stronger after T102S- and K99A-stimulation compared to WT peptide. Thus, although the p23/p21 ratio was consistent with the shorter apparent half lives of the T102S and K99A complexes, the intensity of tyrosine phosphorylation and the prolonged kinetics correlated with the proliferative response.

### Relationships between Half-Life of TCR-pMHC Complexes, cSMAC Formation, and Integrated Signal

These seemingly paradoxical results showing, for example, that the K99A peptide does not induce efficient cSMAC formation but elicits a greater proliferative response compared to the WT peptide (which induces a cSMAC) suggested a complex interplay between competing phenomena that was difficult to intuit. We therefore undertook a computational study to gain further insights.

Because T cell activation requires prolonged signaling, we assumed that the integrated amount of signaling over time would correlate with proliferation. How the integrated amount of signal depends upon the on and off rates characterizing TCR-pMHC binding and cSMAC formation was then analyzed. Because the role of the cSMAC in regulating TCR degradation is still unresolved, we examined the consequences of two different hypotheses. In the first hypothesis, no special assumption was made regarding where receptor degradation can occur. Receptor-ligand binding, downstream signaling reactions, and receptor degradation were allowed to occur wherever the appropriate molecules mediating specific chemical reactions encountered each other. In the second hypothesis, as per suggestions in the literature (Campi et al., 2005; Yokosuka et al., 2005), it was a priori assumed that receptor degradation could occur only in the cSMAC.

Computational investigation of either hypothesis requires a model for TCR signaling. The TCR signaling model that we studied (described in the Experimental Procedures and Figure S5) is a modification of our previous model (Lee et al., 2003). In the current model, TCR degradation is treated more realistically by incorporating ubiquitination by allowing for the recruitment of the E3 ubiquitin ligase, Cbl, to phosphorylated ZAP-70 and CD3ζ molecules. These interactions resulted in ubiquitination, and only ubiquitinated receptors were subject to degradation. Thus, degradation is naturally linked to the level and concentration of phosphorylated substrates. In the first model, no restriction was imposed as to where Cbl could interact with receptors. In the second hypothesis, it was assumed that these processes can occur only in the cSMAC.

Calculations were first carried out to examine the effects of  $k_{off}$  and cSMAC formation on the integrated signal, fixing the on rate for TCR-pMHC binding. We studied two situations, one where a cSMAC was allowed to form regardless of the value of  $k_{off}$ , and the other where the cSMAC never forms. Consider first representative data for the first hypothesis where no special assumption was made about where receptor degradation can occur (Figure 6A). These

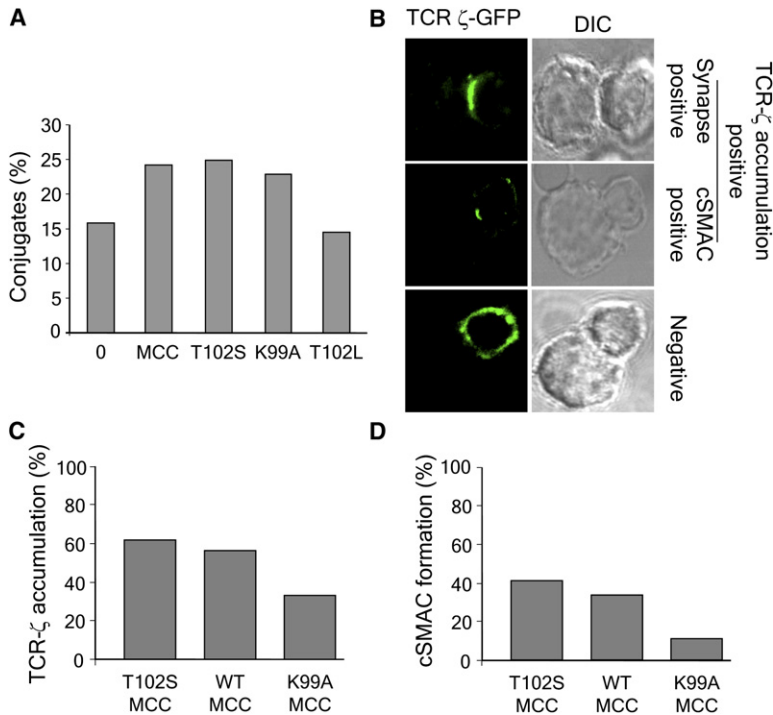


**Figure 4. Conjugate and Immunological Synapses Formation Induced by WT, K99A, and T102S MCC Peptides**

(A) CD4<sup>+</sup> AND T cells were labeled with CFSE and incubated for 30 min with peptide-pulsed, Cell Trace-calcein-labeled CH27 cells. Cells were then gently washed and conjugate formation assessed by flow cytometry. The percentage of T cells forming conjugates is presented as percentage of total T cells. A representative of three independent experiments is shown. (B–D) CD4<sup>+</sup> AND T cells were retrovirally transduced with GFP-TCR- $\zeta$  and sorted for GFP expression. T cells were incubated with CH27 cells pulsed with 30  $\mu$ M of the indicated peptide. After 30 min, cells were fixed, mounted on poly-L-lysine-treated slides, and analyzed by confocal microscopy. More than 100 individual T cell-CH27 conjugates collected in three independent experiments were assessed for each tested peptide. Examples of how cell conjugates were scored for TCR- $\zeta$  accumulation at the contact site are shown in (B). The percentages of T cells accumulating TCR- $\zeta$  at the contact site (C) and forming cSMACs (D) are presented as percentage of total conjugates analyzed. A representative of three independent experiments is shown.

results showed that, for ligands that bind the TCR with a long half-life, cSMAC formation led to a reduced amount of integrated signal. On the other hand, for ligands that bind the TCR with a short half-life, cSMAC formation is predicted to lead to an increase in the total integrated signal.

Analyses of our results showed that, for ligands with long half-lives (small  $k_{off}$ ), receptors are triggered efficiently without need for clustering in the cSMAC (Figure S6A). However, we found that, for these ligands, cSMAC formation increases the rate of degradation (Figure S7A). Our analysis showed that this is because concentrating receptors in one spatial location (cSMAC) enhances the ability of Cbl to ubiquitinate substrates (Figure S8). Thus, the lower total integrated signal seen for strong ligands when cSMACs can form is explained by increased receptor downregulation (Figure S7A).

At larger values of  $k_{off}$  (half-life is short), this was reversed. Because weakly binding ligands did not trigger TCR efficiently, clustering of receptors, ligands, and kinases in the cSMAC aids in the generation of phosphorylated receptors and activated signaling intermediates because the enhanced concentration increased receptor occupancy and rates of phosphorylation (Figure S6B). For these qualities of ligand, the integrated signal was distinctly smaller when the cSMAC did not form (Figure S7B). Because these ligands induce lower amounts of phosphorylation and p23/p21 ratio (data not shown), the effects of cSMAC formation on signaling dominated over the effects of cSMAC formation on receptor downregulation. Importantly, the two curves in Figure 6A (with and without cSMAC formation) intersect at a particular value of  $k_{off}$

where the advantages and disadvantages of cSMAC formation are balanced.

A critical issue in the interpretation of these simulations for the first hypothesis is the threshold value of  $k_{off}$  required to stimulate cSMAC formation (Grakoui et al., 1999; Sumen et al., 2004) and the relationship between this threshold and the point at which the two integrated signaling curves intersect. If the value of  $k_{off}$  that triggers cSMAC formation does not correspond to the intersection point, the amount of integrated signal will exhibit a discontinuous change when T cells are stimulated by a ligand that is slightly weaker than that required for efficient cSMAC formation. For example, if the threshold value of  $k_{off}$  that triggers cSMAC formation is higher (to the right) than the intersection point, the amount of integrated signal will precipitously decrease for a ligand that has a value of  $k_{off}$  just above this threshold required for forming cSMACs. If the threshold value of  $k_{off}$  that triggers cSMAC formation is smaller (to the left) of the intersection point, the amount of integrated signal will abruptly increase for ligands whose binding to TCR has a value of  $k_{off}$  just above this threshold. Our experimental results showing that K99A elicits a stronger proliferative response than MCC, but does not form cSMACs efficiently, suggests that, if the first model is valid, the threshold for cSMAC formation lies to the left of the intersection point for AND T cells. It also suggests that if T cells stimulated by K99A could be manipulated to efficiently form a cSMAC, the integrated signal (i.e., stimulatory capacity) would be lower.

Calculations for the second hypothesis, where it is assumed that receptor downregulation can occur only in the cSMAC, are shown in Figure 6B. In contrast to

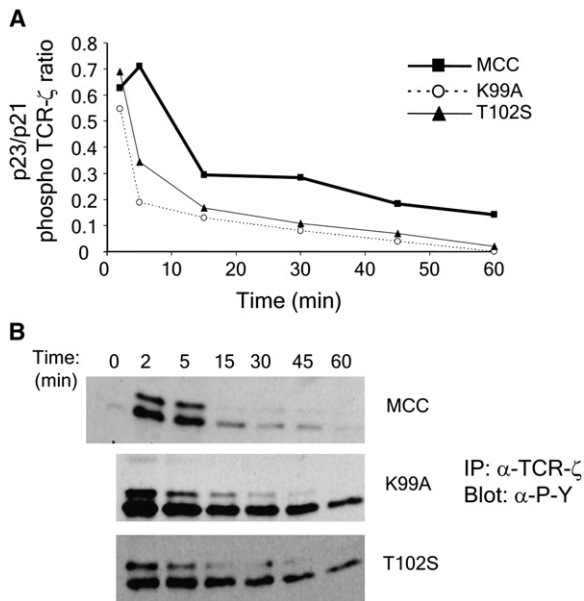


**Figure 5. Kinetics of TCR- $\zeta$  Phosphorylation in AND Cells upon Stimulation with WT, K99A, and T102S MCC**

Rested AND CD4<sup>+</sup> T cells were stimulated with CH27 cells loaded with 10  $\mu$ M of the indicated peptide for the indicated times. Upon stimulation, cells were lysed, and TCR- $\zeta$  was immunoprecipitated, immunoblotted for tyrosine phosphorylation, and analyzed by densitometry.

(A) p23/p21 ratio after WT, K99A, and T102S MCC stimulation over time.

(B) The anti-phospho-tyrosine western blots analyzed by densitometry. A representative of four independent experiments is shown.

Figure 6A, the curves with and without cSMAC formation do not cross at any value of  $k_{off}$ . In this model, cSMAC formation is predicted to reduce the amount of integrated signal for all antigen qualities. Thus, this hypothesis is also consistent with our experimental data on K99A: it suggests that the inability to form a cSMAC will enhance stimulatory capacity regardless of TCR-pMHC off rate. Differences between the results in Figures 6A and 6B suggest a way to distinguish between the two hypotheses. For example, if a sufficiently weak ligand that normally cannot stimulate cSMAC formation could be coerced to form a cSMAC and the stimulatory potency increased, then the first hypothesis would be correct.

**NKG2D-Mediated cSMAC Formation Reduces the Proliferative Response to K99A**

Previously, we showed that the engagement of NKG2D on CD8<sup>+</sup> T cells allows for antigen-independent formation of the cSMAC (Markiewicz et al., 2005). We reasoned, therefore, that expressing NKG2D on AND T cells might induce cSMAC formation and thereby enable us to test whether the stimulatory potency of K99A would be reduced by cSMAC formation. AND T cells were doubly transduced with retroviruses containing cDNAs for NKG2D and its required signaling adapter, DAP10-YFP. NKG2D-positive cells were conjugated with APCs expressing the NKG2D

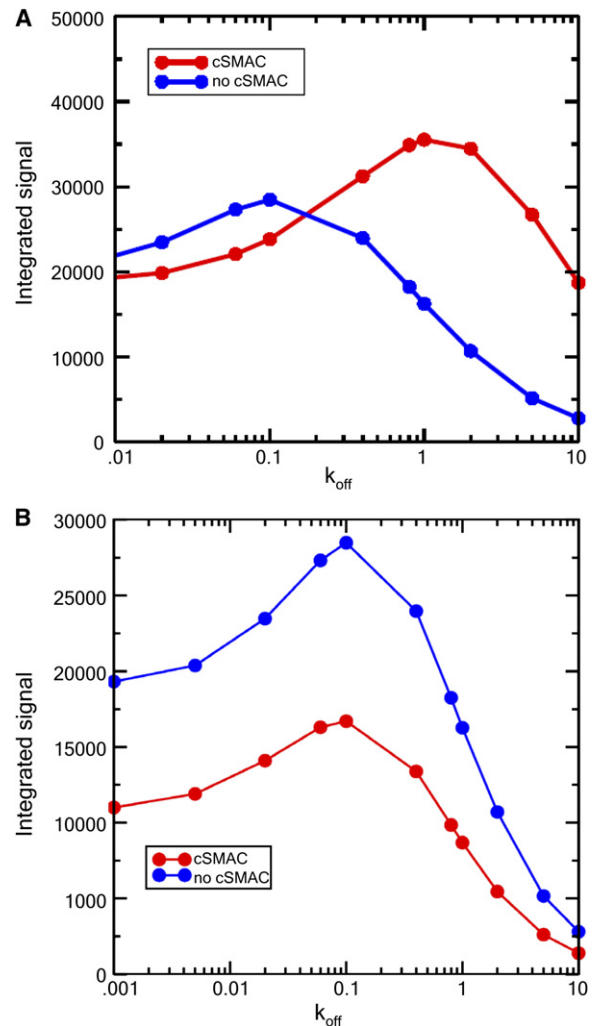


**Figure 6. Dependence of Integrated Signal on Antigen Quality**

(A) Results for the first hypothesis described in the text. Data for calculations are compared for two cases, one where a cSMAC (red) is allowed to form regardless of the value of  $k_{off}$  and the other where no cSMAC (blue) is ever present. For small values of  $k_{off}$ , cSMAC formation inhibited the total amount of integrated signal, whereas the opposite was true for ligands that bind TCR weakly. These calculations were carried out with a pMHC density of 1 molecule/ $(\mu\text{m})^2$ . Higher pMHC densities (e.g., 10 molecules/ $(\mu\text{m})^2$ ) did not change the qualitative behavior (Figure S11). These calculations were carried out for a value (Li et al., 2004) of  $k_{on}$  equal to 2200  $\text{M}^{-1} \text{s}^{-1}$ .

(B) Results for the second hypothesis described in the text. Integrated signal from a model (red) where the cSMAC serves as a site for degradation only is compared with the situation where there is no cSMAC formation (blue). All parameters are the same as in (A). The signal is always higher when there is no cSMAC formation and there is no intersection point, as in (A).

ligand, Rae-1 $\epsilon$ , preincubated with the K99A peptide. As expected, NKG2D engagement strongly enhanced cSMAC formation both in the presence and absence of K99A peptide (Figures 7A–7C). Importantly, expression of NKG2D significantly reduced the level of proliferation induced by K99A (Figure 7D). This supports our prediction

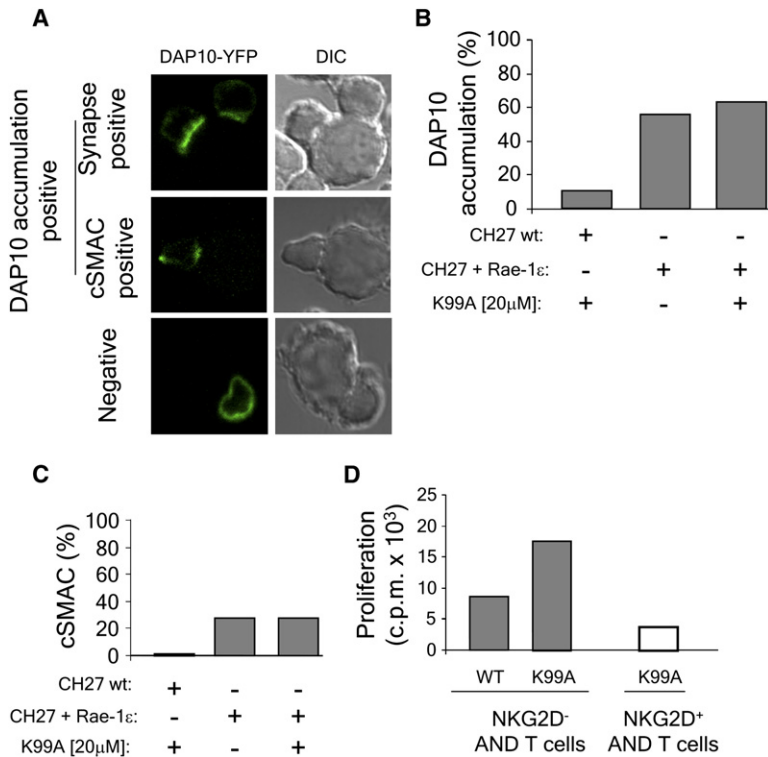


**Figure 7. Coerced cSMAC Formation Inhibits the Proliferative Response of AND T Cells to K99A**

CD4<sup>+</sup> AND T cells were retrovirally transduced with DAP10-YFP and NKG2D and sorted for YFP and NKG2D expression. T cells were incubated, as indicated, with wt CH27 cells or CH27 cells transduced with Rae-1 $\epsilon$ , unpulsed or pulsed with 20  $\mu$ M of the indicated peptide. After 30 min, cells were fixed, mounted on poly-L-lysine-treated slides, and analyzed by confocal microscopy. More than 50 individual T cell-CH27 conjugates obtained in two independent experiments were assessed.

(A) Examples of how cell conjugates were scored for DAP10-YFP accumulation at the contact site are shown.

(B and C) The percentages of T cells accumulating DAP10 at the contact site (B) and forming cSMACs (C) are presented as the percentage of total conjugates analyzed. A representative of two independent experiments is shown.

(D) NKG2D and DAP10-double positive AND T cells (white bar) and WT AND T cells (grey bars) were stimulated with mitomycin C-treated, Rae-1 $\epsilon$ -expressing CH27 cells pulsed with 3  $\mu$ M or 0.1  $\mu$ M (data not shown) of the indicated peptide. The T cell proliferative responses were assessed by the incorporation of [<sup>3</sup>H]thymidine added for the last 18 hr of the stimulation. A representative of two independent experiments is shown.

that the enhanced proliferation seen with K99A is due to its inability to form cSMACs.

#### Relationship between On Rate for TCR-pMHC Binding, cSMAC Formation, and Integrated Signal

We next used our *in silico* model to explore how a higher proliferative response could be induced by the T102S peptide. Tetramer binding experiments suggested that the T102S-MHC complex binds the AND TCR with both a faster relative on and off rate compared to MCC. We therefore used the model to compare the effects of different on rates on the total integrated signal. An example of one of our simulations (following the first hypothesis) where the on rate was increased by a factor of 10 is shown (Figure S9). When the off rate is small and cSMACs form, changing the on rate by a factor of 10 had relatively little effect on the integrated signal. This can be explained by the fact that when the half-life is long, receptor occupancy is largely limited by the availability of pMHC. Under these conditions, enhancing the on rate 10-fold led to only a  $\sim$ 10% change in receptor occupancy. The on rate, however, became important when the off rate was larger (half-life becomes shorter). Under these conditions, pMHC availability is not the limiting factor; increases in the on rate resulted in increased receptor occupancy and increased integrated signal.

These computational results can potentially explain why the T102S peptide, which has a larger apparent off rate and a larger apparent on rate, can stimulate a stronger proliferative response than MCC. The similar affinities of

T102S with MCC suggest that the level of receptor occupancy is similar. But the faster on rate and larger off rate suggests that binding by T102S is much more dynamic than MCC with much greater levels of receptor-ligand exchange. The concomitant increased “serial triggering” could explain the higher integrated signal.

#### DISCUSSION

How different parameters determine the ability of a pMHC molecule to stimulate T cell activation remains unclear. Many studies (Kalergis et al., 2001; Kersh et al., 1998b) have suggested that the off rate characterizing the binding of pMHC ligands to TCR correlates well with its ability to stimulate T cell activation. However, several anomalies have been reported that raise questions about whether this is the only measure of antigen quality. Thus, other parameters and phenomena such as the change in heat capacity upon receptor-ligand binding (Krogsgaard et al., 2003; Qi et al., 2006), serial triggering, synergy between endogenous and agonist ligands (Wulfing et al., 2002; Krogsgaard et al., 2005; Li et al., 2004), and costimulatory interactions (Markiewicz et al., 2005; Puritic et al., 2005; Wulfing et al., 2002) have been implicated in modulating how T cells respond to antigen. Our studies combined *in vitro* and *in silico* investigations to examine the interplay between signaling, peptide quality, and cSMAC formation.

Our results emphasize that the stimulatory potency of a pMHC ligand depends upon many factors and that

agonist quality does not correlate with any one variable. A dramatic example of this is provided by our experimental data for the stimulatory potency of the K99A peptide for AND T cells. This ligand binds the AND TCR with a larger value of the off rate compared to the WT MCC and does not induce cSMAC formation. Yet, it elicited a greater proliferative response. This result raises the question as to whether other APLs classified only by proliferation assays as superagonists might actually be weaker binding ligands that do not induce cSMAC formation resulting in a higher total integrated signal.

Our results suggest that the on rate characterizing TCR-pMHC binding may be important but only when the half-life of the complex is relatively short. When the half-life is long, receptor occupancy is limited by the availability of pMHC molecules, not the on rate. But when half-life is short, a faster on rate will strongly enhance receptor occupancy. Note, however, that these results apply to *in vitro* experiments where the agonist ligand density is relatively high. *In vivo*, antigen is limiting, and in this circumstance synergy between endogenous and agonist ligands could be important for signal amplification (Krogsgaard et al., 2005; Li et al., 2004); this could lead to complications that we have not considered.

When pMHC density is high, as in our *in vitro* experiments, endogenous ligands are not necessary for receptor triggering. In this circumstance, competition between serial triggering and kinetic proofreading is predicted to lead to an optimal half-life; i.e., pMHC that bind TCR with this half-life are most stimulatory. The AND TCR is not a physiological TCR and selects poorly on the k haplotype. This suggests that the half-life of the AND TCR for MCC peptide bound to I-A<sup>k</sup> might be higher than optimal. Thus, it is perhaps not surprising that T102S, which binds the AND TCR with a shorter half-life compared to MCC, enhances signaling.

One idea emerging from our studies is that the dependence of cSMAC formation on TCR-pMHC half-life can modulate how the integrated amount of TCR signaling (and proliferative response) varies with receptor-ligand binding parameters. Our calculations showed that, for ligands that bind TCR sufficiently strongly, weaker ligands that do not induce cSMAC formation should induce greater proliferative responses. This explanation for our experimental data on AND T cells stimulated by the K99A peptide are clearly supported by our results showing the reduced stimulatory potency of this peptide upon forcing cSMAC formation by expression of NKG2D. The results of this experiment are especially striking because NKG2D is thought to function as a costimulator to enhance signaling through the TCR.

We should also note that the results of the experiment with NKG2D are consistent with both hypotheses whose consequences we examined by using *in silico* modeling. If the half-life for TCR-pMHC complexes is relatively long, a ligand that cannot induce cSMAC formation will result in a larger integrated signal. This result is also consistent with our previously reported experimental results that showed that disruption of cSMAC formation resulting from

CD2AP deficiency resulted in prolonged signaling and a more robust response when T cells were stimulated by a strong agonist (Lee et al., 2003).

Recent work that used single-molecule imaging of T cells interacting with artificial lipid bilayers loaded with strong agonists and inhibitors of actin polymerization and antibodies that block TCR engagement suggest that signaling occurs mainly at the periphery of the contact area in microclusters (Campi et al., 2005; Mossman et al., 2005; Varma et al., 2006; Yokosuka et al., 2005). Consistent with this result, our computer simulations showed that, for high-affinity agonists, TCRs are efficiently triggered in the periphery without need for clustering of molecules in the cSMAC. Our computational model, however, does not explicitly treat microclusters because it is a coarse-grained model that describes species in terms of concentrations. However, we expect the qualitative results reported by us to be similar if we were to carry out a simulation where individual receptor-ligand interactions and their clusters were treated explicitly. This is because, for strong agonists, we find that receptor triggering occurs efficiently in the pSMAC in our coarse-grained calculations just as is posited to occur in microclusters.

The paucity of phosphotyrosine staining in the cSMAC when T cells are stimulated by strong agonists has been interpreted to signify that the cSMAC functions only as a site of degradation (Mossman et al., 2005; Campi et al., 2005). Our computational results suggest that these past studies and the results reported by us in the present paper cannot unequivocally reach this conclusion because the situation could be different for weak ligands that are yet to be studied.

The major difference between the two hypotheses that we examined is manifested in the response to a peptide with a much shorter half-life than any we have tested. For peptides with very short half-lives, the first hypothesis (wherein no assumption is made about where degradation may occur) predicts that if cSMAC formation could occur, it would result in enhanced recognition of weak peptides. In contrast, the second hypothesis (where it is posited that degradation can occur only in the cSMAC) predicts that cSMAC formation will always weaken signaling. Our efforts to distinguish between these two hypotheses in this way are currently constrained by the fact that no adequate weak peptides are known for the AND TCR system.

It could be argued that the weak peptides that would distinguish between these two models are not physiologically relevant, because they would probably be too weak to activate T cells. However, it has recently become clear that endogenous peptides that are unable to stimulate T cell activation on their own are likely to play significant roles in TCR triggering (Krogsgaard et al., 2005; Li et al., 2004; Yachi et al., 2006). The presence or absence of cSMACs could potentially determine the stimulatory capacity of such endogenous peptides at late time points in T cell signaling. This also raises important issues about *in vivo* situations where mixtures of both weak and strong ligands are present. Furthermore, the function of the cSMAC for less sensitive naive T cells requires careful examination.



Our understanding of the function of the cSMAC is still evolving. We hope that continued synergy between modeling and experiments will help unravel this enigma.

## EXPERIMENTAL PROCEDURES

### Mice

AND TCR transgenic mice (B6;SJL-Tg(TcrAND)53Hed/J) and B10.BR mice (B10.BR-*H2<sup>d</sup>*-*H2-T18<sup>a</sup>*/SgSnJ) were purchased from The Jackson Laboratory. 5C.C7 TCR transgenic mice (5C.C7 TCRtg RAG-2<sup>-/-</sup>-*H-2<sup>b</sup>*) were obtained from Taconic Farms. Mice were maintained under pathogen-free conditions in the Washington University animal facilities in accordance with institutional guidelines.

### MCC Peptides

Wild-type and mutated moth cytochrome C (MCC) peptides 88–103 were synthesized by standard F-moc chemistry. The peptides were purified to homogeneity by reverse-phase HPLC, and their composition was confirmed by mass spectrometry and amino acid analysis (Washington University Mass Spectrometry Facility, St. Louis, MO).

### T Cell Purification

For purification of splenic T cells, splenocytes were depleted of CD8<sup>+</sup>, MHC class II-positive, and immunoglobulin-positive cells by antibody-mediated nanoparticle negative selection (EasySep CD4<sup>+</sup> negative selection cocktail, StemCell Technologies). The CD4<sup>+</sup> T cells were used immediately as naive T cells or stimulated for 4 days with irradiated B10.BR splenocytes and MCC peptide, rested for 2 days, and then used.

### TCR Downregulation

AND T cells were stimulated for 3 hr, in a 1:1 ratio, with peptide pulsed or unpulsed CH27 I-E<sup>k</sup> cells. Upon stimulation, cells were pelleted and treated with trypsin-EDTA to break cell conjugates, washed, and labeled with FITC-conjugated anti-CD4 and PE-conjugated anti-V $\beta$ 3 antibodies (BD PharMingen). V $\beta$ 3 surface expression was assessed by flow cytometry (FACScan, BD Biosciences) on CD4-positive gated cells. Data was analyzed by WinMDI 2.8 software (<http://facs.scripps.edu/software.html>) or CellQuest (BD PharMingen).

### Cell Lysis, Immunoprecipitation, and Western Blotting

AND T cells were pretreated with cyclohexamide for 45 minutes and stimulated with an equal number of unpulsed or peptide-pulsed CH27 I-E<sup>k</sup> cells. After stimulation, cells were lysed for 10 min on ice in 1% NP-40-containing lysis buffer and cleared by centrifugation. For TCR degradation assays, postnuclear supernatants were resolved on SDS-PAGE under reducing conditions, transferred to nitrocellulose membranes, and immunoblotted with an anti-TCR- $\zeta$  antiserum. For TCR- $\zeta$  phosphorylation, postnuclear supernatants were immunoprecipitated with an anti-TCR- $\zeta$  antiserum, resolved on SDS-PAGE, transferred to nitrocellulose membranes, and immunoblotted with an anti-phosphotyrosine antibody (clone 4G10; Upstate Biotechnology). Blots were visualized with ECL Western blotting kit (Pierce). Densitometry was performed with IPLab software (Scanalytics).

### T Cell Proliferation Assays

Naive or rested CD4<sup>+</sup> AND or 5C.C7 T cells were stimulated for 48 hr with irradiated B10.BR cells and various amounts of peptides, pulsed with 1  $\mu$ Ci of [<sup>3</sup>H]thymidine/well, harvested 16 h later, and scintillation counted. Cells were labeled with CFSE, stimulated for 3 days with irradiated B10.BR splenocytes prepulsed with peptides, and assessed for CFSE staining by flow cytometry.

### Transfection and Retroviral Transduction

The Plat E ecotropic packaging cell line was transfected with a TCR- $\zeta$ -GFP retroviral construct (kindly provided by M. Davis, Stanford University) or a mixture of NKG2D and DAP10-YFP retroviral constructs. AND

T cells were stimulated with irradiated B10.BR splenocytes and 10  $\mu$ M MCC peptide. At 18 and 42 hr after stimulation, T cells were incubated for 4 hr with the viral supernatants upon spinfection for 45 min in the presence of Lipofectamine 2000 (Invitrogen). At day 4 after stimulation, GFP-positive T cells were sorted with FACS Vantage flow sorter (BD Biosciences) at the Washington University Pathology Cell Sorting Facility. After NKG2D/DAP10-YFP double transduction, cells were stained with a PE-labeled anti-NKG2D antibody, and YFP-positive, PE-positive cells were sorted and used for further experimentation.

### T Cell-APC Conjugate Formation

T cells and APCs were labeled with CFSE and Cell Trace calcein red-orange, AM (Molecular Probes), respectively, and incubated for 30 min to allow conjugate formation. Cells were then gently washed and conjugate formation was assessed by flow cytometry as the ratio of CFSE/Cell Trace double-positive cells to total CFSE-positive cells. Data were analyzed by WinMDI 2.8 software (<http://facs.scripps.edu/software.html>) or CellQuest (BD PharMingen).

### IS and cSMAC Formation

Sorted retrovirally transduced AND T cells were incubated with peptide loaded or unloaded CH27 I-E<sup>k</sup> cells for 30 min. Cells were then fixed and mounted on coverslips, and confocal images were taken with a Zeiss LSM510 confocal microscope. Unprocessed images were scored by ImageJ software (NIH, Bethesda, MD, <http://rsb.info.nih.gov/ij/>, 1997–2006), as described in the text.

### Tetramer Production, Tetramer Staining, and Tetramer-Decay Experiments

I-E<sup>k</sup>-MCC tetramers (with WT, K99A, or T102S MCC) were generated as described previously (Gutgemann et al., 1998). For equilibrium staining, AND T cells were stained with I-E<sup>k</sup>-MCC tetramers for 3 hr at 10°C, washed twice, resuspended in FACS buffer, and analyzed by flow cytometry. For relative  $K_{off}$  measurements, AND T cells were stained for 3 hr at 4°C, washed twice, resuspended in FACS buffer in the presence of 100 mg/ml of 14.4.4 antibody, and incubated at 4°C to allow tetramer decay. At specific time points, cells were removed and analyzed for staining by flow cytometry. A tetramer with an irrelevant peptide bound (Hb) was used as a negative control. Mean fluorescence at each time point was calculated by subtracting the mean fluorescence of the negative control and then normalizing to the fluorescence at time zero.

### The Computational Model

A continuum model that parallels and complements our previous stochastic models (Lee et al., 2003) was developed. This enables us to readily examine large systems under diverse conditions and exhaustively examine the sensitivity of the model to values of unknown parameters. However, stochastic models (Lee et al., 2003; Li et al., 2004) are necessary if the copy number of certain species is very small. Because most in vitro experiments are carried out with a rather high antigen dose (e.g., concentration of agonist peptides loaded on supported lipid bilayers is 1–100 molecules/ $\mu$ m<sup>2</sup> [Grakoui et al., 1999]), use of the continuum model is appropriate. Varying the densities of various species led to qualitatively similar results over a range of values, and the effects of fluctuations for low pMHC densities and small values of the off rate were not large for the conditions of interest in this paper (Supplemental Data and Figure S10).

In the model, the membrane-associated and cytosolic molecules undergo biochemical reactions according to the signaling cascade shown in Figure S5. As described in the text, receptor degradation is treated more accurately with incorporation of ubiquitination. Some details found not to affect qualitative results of interest in this paper were not incorporated in the present study (feedback loops regulating Lck activity [Altan-Bonnet and Germain, 2005; Stefanova et al., 2003] and downstream signaling molecules [Ras, Rac, etc., that are downstream of ZAP70 activation]).

cSMAC is modeled as described previously (Lee et al., 2003). We link cSMAC formation to downstream signaling by turning on a potential field that acts on certain species and drives them to form a cSMAC when activated ZAP70 exceeds a threshold. The spatially varying potential field is a coarse-grained representation of forces (derivative of a potential) that direct cSMAC formation. The magnitude of the potential is chosen so that a cSMAC forms in a few (~5) minutes. The depth and spatial variation of this potential field determine the rate of cSMAC formation and the concentration of species therein.

The spatio-temporal distribution of each species varies because of diffusion, biochemical reactions that are part of the signaling cascade, and convective motion if a cSMAC is formed. The relevant equations are provided in the Supplemental Data. The numerical methods used to solve the large set of partial differential equations are provided in the Supplemental Data, which also contains a list of parameters used to carry out our calculations and a discussion of our relatively extensive parameter sensitivity studies.

#### Supplemental Data

Supplemental Data include eleven figures, two tables, two movies, and Experimental Procedures and can be found with this article online at <http://www.immunity.com/cgi/content/full/26/3/345/DC1/>.

#### ACKNOWLEDGMENTS

We thank M. Dustin for fruitful discussions. This research is supported by the NIH (grants AI034094, AI057966, and AI071195-01).

Received: May 10, 2006

Revised: December 15, 2006

Accepted: January 23, 2007

Published online: March 8, 2007

#### REFERENCES

- Altan-Bonnet, G., and Germain, R.N. (2005). Modeling T cell antigen discrimination based on feedback control of digital ERK responses. *PLoS Biol.* 3, e356. 10.1371/journal.pbio.0030356.
- Bachmann, M.F., Oxenius, A., Speiser, D.E., Mariathasan, S., Hengartner, H., Zinkernagel, R.M., and Ohashi, P.S. (1997). Peptide-induced T cell receptor down-regulation on naive T cells predicts agonist/partial agonist properties and strictly correlates with T cell activation. *Eur. J. Immunol.* 27, 2195–2203.
- Berg, L.J., Pullen, A.M., Fazekas de St Groth, B., Mathis, D., Benoist, C., and Davis, M.M. (1989). Antigen/MHC-specific T cells are preferentially exported from the thymus in the presence of their MHC ligand. *Cell* 58, 1035–1046.
- Campi, G., Varma, R., and Dustin, M.L. (2005). Actin and agonist MHC-peptide complex-dependent T cell receptor microclusters as scaffolds for signaling. *J. Exp. Med.* 202, 1031–1036.
- Evavold, B.D., Sloan-Lancaster, J., and Allen, P.M. (1993). Tickling the TCR: selective T-cell functions stimulated by altered peptide ligands. *Immunol. Today* 14, 602–609.
- Gonzalez, P.A., Carreno, L.J., Coombs, D., Mora, J.E., Palmieri, E., Goldstein, B., Nathenson, S.G., and Kalergis, A.M. (2005). T cell receptor binding kinetics required for T cell activation depend on the density of cognate ligand on the antigen-presenting cell. *Proc. Natl. Acad. Sci. USA* 102, 4824–4829.
- Grakoui, A., Bromley, S.K., Sumen, C., Davis, M.M., Shaw, A.S., Allen, P.M., and Dustin, M.L. (1999). The immunological synapse: a molecular machine controlling T cell activation. *Science* 285, 221–227.
- Gutgemann, I., Fahrner, A.M., Altman, J.D., Davis, M.M., and Chien, Y.H. (1998). Induction of rapid T cell activation and tolerance by systemic presentation of an orally administered antigen. *Immunity* 8, 667–673.
- Itoh, Y., Hemmer, B., Martin, R., and Germain, R.N. (1999). Serial TCR engagement and down-modulation by peptide:MHC molecule ligands: relationship to the quality of individual TCR signaling events. *J. Immunol.* 162, 2073–2080.
- Kalergis, A.M., Boucheron, N., Doucey, M.A., Palmieri, E., Goyarts, E.C., Vegh, Z., Luescher, I.F., and Nathenson, S.G. (2001). Efficient T cell activation requires an optimal dwell-time of interaction between the TCR and the pMHC complex. *Nat. Immunol.* 2, 229–234.
- Kaye, J., Hsu, M.L., Sauron, M.E., Jameson, S.C., Gascoigne, N.R., and Hedrick, S.M. (1989). Selective development of CD4+ T cells in transgenic mice expressing a class II MHC-restricted antigen receptor. *Nature* 341, 746–749.
- Kersh, E.N., Shaw, A.S., and Allen, P.M. (1998a). Fidelity of T cell activation through multistep T cell receptor zeta phosphorylation. *Science* 281, 572–575.
- Kersh, G.J., Kersh, E.N., Fremont, D.H., and Allen, P.M. (1998b). High- and low-potency ligands with similar affinities for the TCR: the importance of kinetics in TCR signaling. *Immunity* 9, 817–826.
- Krogsgaard, M., Prado, N., Adams, E.J., He, X.L., Chow, D.C., Wilson, D.B., Garcia, K.C., and Davis, M.M. (2003). Evidence that structural rearrangements and/or flexibility during TCR binding can contribute to T cell activation. *Mol. Cell* 12, 1367–1378.
- Krogsgaard, M., Li, Q.J., Sumen, C., Huppa, J.B., Huse, M., and Davis, M.M. (2005). Agonist/endogenous peptide-MHC heterodimers drive T cell activation and sensitivity. *Nature* 434, 238–243.
- Krummel, M.F., Sjaastad, M.D., Wulfiging, C., and Davis, M.M. (2000). Differential clustering of CD4 and CD3zeta during T cell recognition. *Science* 289, 1349–1352.
- Lee, K.H., Holdorf, A.D., Dustin, M.L., Chan, A.C., Allen, P.M., and Shaw, A.S. (2002). T cell receptor signaling precedes immunological synapse formation. *Science* 295, 1539–1542.
- Lee, K.H., Dinner, A.R., Tu, C., Campi, G., Raychaudhuri, S., Varma, R., Sims, T.N., Burack, W.R., Wu, H., Wang, J., et al. (2003). The immunological synapse balances T cell receptor signaling and degradation. *Science* 302, 1218–1222.
- Li, Q.J., Dinner, A.R., Qi, S., Irvine, D.J., Huppa, J.B., Davis, M.M., and Chakraborty, A.K. (2004). CD4 enhances T cell sensitivity to antigen by coordinating Lck accumulation at the immunological synapse. *Nat. Immunol.* 5, 791–799.
- Lin, J., Miller, M.J., and Shaw, A.S. (2005). The c-SMAC: sorting it all out (or in). *J. Cell Biol.* 170, 177–182.
- Lyons, D.S., Lieberman, S.A., Hampl, J., Boniface, J.J., Chien, Y., Berg, L.J., and Davis, M.M. (1996). A TCR binds to antagonist ligands with lower affinities and faster dissociation rates than to agonists. *Immunity* 5, 53–61.
- Madrenas, J., Wange, R.L., Wang, J.L., Isakov, N., Samelson, L.E., and Germain, R.N. (1995). Zeta phosphorylation without ZAP-70 activation induced by TCR antagonists or partial agonists. *Science* 267, 515–518.
- Markiewicz, M.A., Carayannopoulos, L.N., Naidenko, O.V., Matsui, K., Burack, W.R., Wise, E.L., Fremont, D.H., Allen, P.M., Yokoyama, W.M., Colonna, M., and Shaw, A.S. (2005). Costimulation through NKG2D enhances murine CD8+ CTL function: similarities and differences between NKG2D and CD28 costimulation. *J. Immunol.* 175, 2825–2833.
- Matsui, K., Boniface, J.J., Steffner, P., Reay, P.A., and Davis, M.M. (1994). Kinetics of T-cell receptor binding to peptide/I-Ek complexes: correlation of the dissociation rate with T-cell responsiveness. *Proc. Natl. Acad. Sci. USA* 91, 12862–12866.
- Monks, C.R., Freiberg, B.A., Kupfer, H., Sciaky, N., and Kupfer, A. (1998). Three-dimensional segregation of supramolecular activation clusters in T cells. *Nature* 395, 82–86.
- Mossman, K.D., Campi, G., Groves, J.T., and Dustin, M.L. (2005). Altered TCR signaling from geometrically repatterned immunological synapses. *Science* 310, 1191–1193.

- Purtic, B., Pitcher, L.A., van Oers, N.S., and Wulfig, C. (2005). T cell receptor (TCR) clustering in the immunological synapse integrates TCR and costimulatory signaling in selected T cells. *Proc. Natl. Acad. Sci. USA* *102*, 2904–2909.
- Qi, S., Krogsgaard, M., Davis, M.M., and Chakraborty, A.K. (2006). Molecular flexibility can influence the stimulatory ability of receptor-ligand interactions at cell-cell junctions. *Proc. Natl. Acad. Sci. USA* *103*, 4416–4421.
- Reay, P.A., Kantor, R.M., and Davis, M.M. (1994). Use of global amino acid replacements to define the requirements for MHC binding and T cell recognition of moth cytochrome c (93-103). *J. Immunol.* *152*, 3946–3957.
- Rogers, P.R., Grey, H.M., and Croft, M. (1998). Modulation of naive CD4 T cell activation with altered peptide ligands: the nature of the peptide and presentation in the context of costimulation are critical for a sustained response. *J. Immunol.* *160*, 3698–3704.
- Seder, R.A., Paul, W.E., Davis, M.M., and Fazekas de St Groth, B. (1992). The presence of interleukin 4 during in vitro priming determines the lymphokine-producing potential of CD4+ T cells from T cell receptor transgenic mice. *J. Exp. Med.* *176*, 1091–1098.
- Sloan-Lancaster, J., Shaw, A.S., Rothbard, J.B., and Allen, P.M. (1994). Partial T cell signaling: altered phospho-zeta and lack of zap70 recruitment in APL-induced T cell anergy. *Cell* *79*, 913–922.
- Stefanova, I., Hemmer, B., Vergelli, M., Martin, R., Biddison, W.E., and Germain, R.N. (2003). TCR ligand discrimination is enforced by competing ERK positive and SHP-1 negative feedback pathways. *Nat. Immunol.* *4*, 248–254.
- Sumen, C., Dustin, M.L., and Davis, M.M. (2004). T cell receptor antagonism interferes with MHC clustering and integrin patterning during immunological synapse formation. *J. Cell Biol.* *166*, 579–590.
- Valitutti, S., Muller, S., Cella, M., Padovan, E., and Lanzavecchia, A. (1995). Serial triggering of many T-cell receptors by a few peptide-MHC complexes. *Nature* *375*, 148–151.
- Varma, R., Campi, G., Yokosuka, T., Saito, T., and Dustin, M.L. (2006). T cell receptor-proximal signals are sustained in peripheral microclusters and terminated in the central supramolecular activation cluster. *Immunity* *25*, 117–127.
- Wulfig, C., Rabinowitz, J.D., Beeson, C., Sjaastad, M.D., McConnell, H.M., and Davis, M.M. (1997). Kinetics and extent of T cell activation as measured with the calcium signal. *J. Exp. Med.* *185*, 1815–1825.
- Wulfig, C., Sumen, C., Sjaastad, M.D., Wu, L.C., Dustin, M.L., and Davis, M.M. (2002). Costimulation and endogenous MHC ligands contribute to T cell recognition. *Nat. Immunol.* *3*, 42–47.
- Yachi, P.P., Ampudia, J., Zal, T., and Gascoigne, N.R. (2006). Altered peptide ligands induce delayed CD8-T cell receptor interaction—a role for CD8 in distinguishing antigen quality. *Immunity* *25*, 203–211.
- Yokosuka, T., Sakata-Sogawa, K., Kobayashi, W., Hiroshima, M., Hashimoto-Tane, A., Tokunaga, M., Dustin, M.L., and Saito, T. (2005). Newly generated T cell receptor microclusters initiate and sustain T cell activation by recruitment of Zap70 and SLP-76. *Nat. Immunol.* *6*, 1253–1262.